

Initial Attitude Estimation of Tactical Grade Inertial Measurement Unit for Airborne Environmental Camera

Hyo-Sung Ahn, Chang-Hee Won, Douglas Olsen, Richard Schultz, Arnold Johnson, William Semke, George A. Seielstad

University of North Dakota

Chuck Wivell

DIGIT Inc.

Abstract

The initial attitude estimation of the airborne navigation system greatly affects the overall attitude accuracy. The initial alignment depends on the inertial measurement unit's performance. In the case of the tactical grade inertial measurement unit, even though tilt angles can be estimated relatively accurately by using accelerometer outputs, it is difficult to determine the azimuth angle with gyroscope outputs because of the uncompensated bias components. Therefore it is necessary to use the appropriate calibration method in order to compensate biases. In this paper, we propose a new method to determine the uncompensated biases. Furthermore, the measurement error covariance is difficult to determine in the navigation error equation because of the navigation frame disturbance. This paper proposed to use the adaptive filtering method to calculate the measurement error covariance matrix. Simulation and laboratory experiments were performed to show the effectiveness of the proposed method of determining uncompensated bias and the adaptive filtering method of calculating the measurement error covariance.

1. INTRODUCTION

Airborne Environmental Research Observational Camera (AEROCam) is an aerial multi-spectral camera imaging system being developed at the University of North Dakota with DIGIT Inc. The remote images portray photographs of reflective radiation in the red, green, blue, and near infrared bands of the electromagnetic spectrum. The purpose behind AEROCam is that the system is designed to fly on a small aircraft to acquire images for use in agriculture, forestry nature conservation, and disaster response. The aerial images give a bird's eye view of the area under investigation. A schematic diagram of AEROCam is shown in Figure 1. The direction of the line of sight of AEROCam is determined by the onboard differential global positioning system (DGPS) and inertial measurement unit (IMU) subsystem. The DGPS/IMU system calculates the attitude transformation matrix using initial attitude alignment information. So the initial alignment of IMU

determines the overall attitude accuracy of the airborne navigation system. The accuracy of coarse alignment is closely related with the IMU performance [1-5].

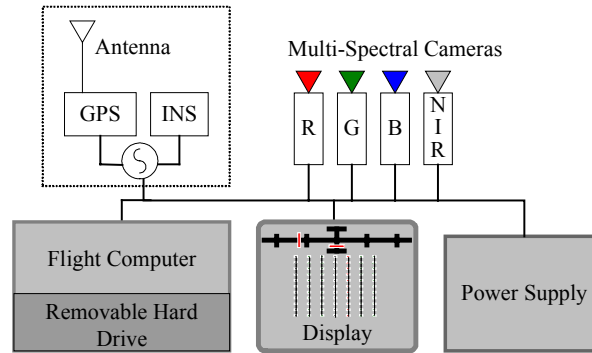


Figure 1. Schematic diagram of AEROCam

For the low-cost tactical grade IMU, azimuth errors of about 30 degrees can occur from the constant bias noise component. When the constant bias is compensated, the turn-on bias component causes about 6~8 degrees azimuth errors. Even if the bias components have been compensated, the random walk noise makes the coarse alignment unreliable. The coarse tilt angle errors depend on the accelerometer bias, and azimuth angle errors depend on the gyroscope bias components. Theoretically, if a gyroscope has 1 degree/hr bias noise at the latitude of 47 degrees, the initial coarse alignment has 7 degrees azimuth error. Because a large constant bias cannot be estimated by the fine alignment algorithm, accurate bias calibration is an indispensable procedure during the initial alignment process [1, 4 and 6]. In order to calibrate the bias components, typically the stored azimuth information is used for the coarse horizontal azimuth alignment [1, 4, 6 and 7]. This stored azimuth information can be determined by attitude sensors such as magnetometers. Using this stored azimuth information, azimuth error is assumed to be zero and tilt errors are found by the alignment procedure. But this stored azimuth method has the disadvantage of using the external reference information. In this paper we find the coarse azimuth angle using only the IMU output.

The accelerometer measurement residual and gyroscope measurement residual are derived from the specific force measurement errors [6 and 8]. If the navigation frame corresponds to the North-East-Down (NED) frame, the navigation frame disturbances have high frequency components. But amplitude and spectral density are time varying and not known accurately [6]. The estimation accuracy depends on the precise knowledge of the model and noise statistics. However accurate noise statistics are difficult to find. Therefore we have applied the adaptive filtering method to model the measurement error covariance automatically. The small error terms such as scale factor errors, misalignment errors and nonlinearity errors can be ignored depending on the cases under investigation. According to a simulation these small error

terms made no difference to the results, thus this paper ignores the scale factor, misalignment error, and nonlinearity error terms. This small error terms however will be considered indirectly within the measurement residuals using an adaptive filter.

The random measurement noise is assumed to be white noise. But amplitude of the noise is larger than the earth rotation rate value sensed by gyroscopes. So it is meaningless to apply the Kalman filter to the raw IMU output data without eliminating the measurement white noise. If the measurement white noise is assumed to be high frequency, we can use the low-pass filter to eliminate the noise. By using the low-pass filter, we can determine the random walk autocorrelation time constant. In general, the random walk noise is assumed to be Gauss-Markov process [1, 6 and 12]. So, in order to model the Gauss-Markov process, autocorrelation time constant of IMU random walk noise has to be determined a priori. The autocorrelation time constant will be determined in this paper by analyzing the IMU outputs in the frequency domain.

The position rate and angle increment in the navigation frame are used for the measurement equation of Kalman filter. These measurements are derived from the specific force error model and angular rate error models. During the stationary alignment procedure, generally zero velocity aiding method is used [1, 6 and 8]. This method uses the zero velocity information of IMU in the navigation frame. So accelerometer measurement data are used to calculate the velocity error in the navigation frame. In general, the gyroscope output is not used in the measurement equations. But some researchers showed that the gyroscope measurement could be used as measurement residuals [6 and 8]. If the angular rate is integrated, the angle increment is measured from the IMU outputs. Stationary IMU gives out angle increment data due to the earth rotation rate. This data is used to determine the measurement residual at the measurement equation. This paper makes the measurement residual from accelerometer X-axis and Y-axis outputs and gyroscope three axis outputs.

Some researchers have suggested the theoretically simple and effective alignment algorithm of the low-cost IMU [1, 8, 13 and 16], but these papers use the simulation IMU output data designed by constant bias noise and random walk noise within certain limits. In real case, IMU outputs include more unpredictable measurement noises such as white noise and random walk noise. So, in the real application, other measurement sensors or landmark points have been used to determine the initial azimuth angle in order to overcome this discrepancy. In Section 2, dynamic equations and measurement equations are introduced, and in Section 3, the results of the frequency domain analysis will be shown. In Section 4, the additive bias calibration method is presented. In Section 5, simulation results are shown in order to verify the code and adaptive filter effectiveness. Also in Section 5, the initial alignment result of DMARS-I-N will be present to verify the theoretical procedure in the practical applications.

2. DYNAMIC EQUATIONS

The states have to be selected by two conditions. One is the IMU performance, and the other is the accuracy of the initial coarse alignment. In the tactical grade IMU, scale factor, misalignment, and nonlinearity are small error terms when they are compared with the bias noise and measurement white noise. So it is useless to include these small error terms in the dynamic equations. But as stated in Section 1, their effect in the measurement error equation will be reflected by adaptive filter. During the initial stationary alignment, the position and velocity are assumed to be known. In the INS error equation, the altitude velocity component is ignored.

Attitude Navigation Equation

The initial stationary fine alignment is made in the motionless state in which position and velocity do not change. Only attitude states are assumed to change because we do not know the true attitude of IMU with respect to NED frame. Therefore, only the attitude navigation equation is used to make the time update. Below attitude navigation equations are propagated using 4th order Runge-Kutta method,

$$\dot{C}_b^n = -\Omega_{b/n}^n C_b^n \quad (1)$$

When the rotation vector, $\underline{\omega}_{b/n}^n$, is given as $\underline{\omega}_{b/n}^n = \underline{\omega}_{i/n}^n - C_b^n \underline{\omega}_{i/b}^b$, the skew symmetric matrix $\Omega_{b/n}^n$ is formed from

$$\Omega_{b/n}^n = \begin{bmatrix} 0 & -\omega_z^n & \omega_y^n \\ \omega_z^n & 0 & -\omega_x^n \\ -\omega_y^n & \omega_x^n & 0 \end{bmatrix} \quad (2)$$

where $\underline{\omega}_{b/n}^n = [\omega_x^n \ \omega_y^n \ \omega_z^n]^T$. The rotation vector $\underline{\omega}_{i/b}^b$ represents the outputs of the strap-down gyros and $\underline{\omega}_{i/n}^n$ represents the theoretical earth rate in NED frame.

INS Error Equations

Here we have modified from Rogers and Farrell's inertial navigation system error model [1 and 6]. The stationary error model augmented with IMU noise models can be written as

$$\begin{bmatrix} \dot{\underline{X}} \\ \dot{\underline{B}} \\ \dot{\underline{R}} \end{bmatrix} = \begin{bmatrix} F & T_1 & T_2 \\ 0_{5 \times 5} & 0_{5 \times 5} & 0_{5 \times 5} \\ 0_{5 \times 5} & 0_{5 \times 5} & T_3 \end{bmatrix} \begin{bmatrix} \underline{X} \\ \underline{B} \\ \underline{R} \end{bmatrix} + G \begin{bmatrix} w_1 \\ 0_{5 \times 1} \\ w_2 \end{bmatrix} \quad (3)$$

The state vector consists of velocity errors in north and east direction (V_N, V_E), attitude errors ($\varepsilon_N, \varepsilon_E, \varepsilon_D$), bias noise components (\underline{B}) of accelerometers and gyroscopes, and random walk noises (\underline{R}) of accelerometers and gyroscopes. These are denoted as

$$\underline{X} = [V_N \ V_E \ \varepsilon_N \ \varepsilon_E \ \varepsilon_D]^T, \underline{B} = [b_{ax} \ b_{ay} \ b_{gx} \ b_{gy} \ b_{gz}]^T, \text{ and } \underline{R} = [RW_{ax} \ RW_{ay} \ RW_{gx} \ RW_{gy} \ RW_{gz}]^T.$$

In Eq. (3),

$$F = \begin{bmatrix} 0 & 2\omega_D & 0 & g & 0 \\ -2\omega_D & 0 & -g & 0 & 0 \\ 0 & \frac{-1}{R} & 0 & \omega_D & 0 \\ \frac{1}{R} & 0 & -\omega_D & 0 & \omega_N \\ 0 & \frac{\tan(\lambda)}{R} & 0 & -\omega_N & 0 \end{bmatrix}, T_1 = T_2 = \begin{bmatrix} C_{11} & C_{12} & 0 & 0 & 0 \\ C_{21} & C_{22} & 0 & 0 & 0 \\ 0 & 0 & C_{11} & C_{12} & C_{13} \\ 0 & 0 & C_{21} & C_{22} & C_{23} \\ 0 & 0 & C_{31} & C_{32} & C_{33} \end{bmatrix}, \text{ and } \underline{G} = \begin{bmatrix} \{C_{bij}^n\}_{i=1,2,j=1,2,3} \\ \{C_{bij}^n\}_{i,j=1,2,3} \\ I_{5 \times 5} \\ I_{5 \times 5} \end{bmatrix} \quad (4)$$

where R is earth radius, $\omega_D = -\omega_{ie} \sin \lambda$, $\omega_N = \omega_{ie} \cos \lambda$ (λ is latitude), $C = \{C_{bij}^n\}_{i,j=1,2,3}$ is the coordinate transformation matrix from IMU body frame to navigation frame and \underline{w}_l is random measurement white noise of accelerometer and gyroscope. \underline{w}_l is a Gaussian white noise with zero mean and varying covariance.

$$T_3 = \begin{bmatrix} -\frac{1}{\tau_{ax}} & 0 & 0 & 0 & 0 \\ 0 & -\frac{1}{\tau_{ay}} & 0 & 0 & 0 \\ 0 & 0 & -\frac{1}{\tau_{gx}} & 0 & 0 \\ 0 & 0 & 0 & -\frac{1}{\tau_{gy}} & 0 \\ 0 & 0 & 0 & 0 & -\frac{1}{\tau_{gz}} \end{bmatrix}, \text{ and } \underline{w}_2 = \begin{bmatrix} \sqrt{2\sigma_{ax}^2 \beta_{ax}} u(t) \\ \sqrt{2\sigma_{ay}^2 \beta_{ay}} u(t) \\ \sqrt{2\sigma_{gx}^2 \beta_{gx}} u(t) \\ \sqrt{2\sigma_{gy}^2 \beta_{gy}} u(t) \\ \sqrt{2\sigma_{gz}^2 \beta_{gz}} u(t) \end{bmatrix} \quad (5)$$

Random walk noise is modeled by Gauss-Markov process as shown in Eq. (5). In Eq. (5), τ_{ax} and τ_{ay} are autocorrelation time constants of accelerometer random walk noises, and τ_{gx} , τ_{gy} and τ_{gz} are autocorrelation time constants of gyroscope random walk noises. And σ is random walk noise standard deviation, β is reciprocal time constant, and $u(t)$ is zero mean unity white Gaussian noise.

Measurement Equations

Accelerometer measurements and gyro measurement are used for the measurement residual of Kalman filter. The error of the calculated acceleration in navigation frame is

$$\delta f^n = - \begin{bmatrix} 0 & -\varepsilon_D & \varepsilon_E \\ \varepsilon_D & 0 & -\varepsilon_N \\ -\varepsilon_E & \varepsilon_N & 0 \end{bmatrix} \begin{bmatrix} 0 \\ 0 \\ g \end{bmatrix} + C_b^n \delta f^b + f_d \quad (6)$$

and the error of the calculated angular rate in navigation frame is

$$\delta \omega = \omega_{i/n}^n - \omega_{i/e}^n = \begin{bmatrix} 0 & -\varepsilon_d & \varepsilon_e \\ \varepsilon_d & 0 & -\varepsilon_n \\ -\varepsilon_e & \varepsilon_n & 0 \end{bmatrix} \begin{bmatrix} \omega_N \\ 0 \\ \omega_D \end{bmatrix} + C_b^n \delta \omega^b + w_d \quad (7)$$

where δf^b are accelerometer measurement uncertainties, $\delta \omega^b$ are gyro measurement uncertainties, and $\omega_{i/e}^n$ are gyro measurements transformed into NED frame. f_d and w_d are navigation frame disturbance errors. These sensor measurement uncertainties and disturbance errors are calculated by adaptive filter as introduced in Section 1. From above two measurement equations, after the linear forces components are integrated, measurement equation can be designed as follow.

$$\underline{y} = \begin{bmatrix} V_N \\ V_E \\ \delta \omega_N \\ \delta \omega_E \\ \delta \omega_D \end{bmatrix} = \begin{bmatrix} 1 & 0 & 0 & 0 & 0 \\ 0 & 1 & 0 & 0 & 0 \\ 0 & 0 & 0 & \omega_D & 0 \\ 0 & 0 & -\omega_D & 0 & \omega_N \\ 0 & 0 & 0 & \omega_N & 0 \end{bmatrix} \begin{bmatrix} X \\ B \\ R \end{bmatrix} + \underline{v} \quad (8)$$

where \underline{v} is measurement noise vector. In Kalman filter, the measurement noise vector is white noise. But as stated in Section 1, it is difficult to estimate the noise magnitude and spectral density function of navigation frame. Measurement noise vector is composed of three different noise components. Primary sources are the small error terms such as misalignment errors and scale factor errors. Secondary sources are the random measurement noises of IMU, which can be modeled as white noise. Third noise is the navigation frame disturbance. Navigation frame disturbance includes the gravity anomaly, and gravity and earth rotation rate variation. Navigation frame disturbance cannot be assumed as white noise. As far as the authors are aware, researchers have not considered navigation frame disturbance. They have either ignored small error terms [1, 7 and 8] or augmented the small error terms as the states [6 and 16]. In this paper, the measurement noise will be a random process including all three error sources. We will determine the error covariance using adaptive filter method. This error covariance will be used in the Kalman filter algorithm as a suboptimal filtering method. The adaptive filter was used because it calculates measurement error covariance matrix by using the real

measurement data. In fact, in real application, the tuning process of the measurement error covariance matrix is troublesome work because the earth rotation rate is very small when compared with the noise magnitude. So when the measurement error covariance was tuned by manual method, it was very difficult to find the proper Kalman gain. For detailed information on the adaptive filter refer to reference text [4].

The actual measurements are accelerometer outputs, gyroscope outputs, zero velocity and earth rotation rates of IMU with respect to NED frame. The velocity errors and angular rate errors in NED frame are used for the measurement. The velocity errors in NED frame are measured from Eq. (6) as

$$(\delta V^n)_{k+1} = (\delta V^n)_k - \Delta t \times \hat{C}_b^n \tilde{f}^b \quad (9)$$

and the angular rate errors in NED frame are measured from Eq. (7) as

$$\delta \omega^n = \omega_{i/n}^n - \hat{C}_b^n \omega_{i/b}^b \quad (10)$$

where, δV^n and $\delta \omega^n$ are used for \tilde{z} in Kalman filter. In accelerometer measurement, the previous velocity is used for the velocity update because accelerometer signals are pulse rates proportional to the measured specific force. So the integrator has to be used for each velocity update. Figure 2 shows the overall initial alignment procedure.

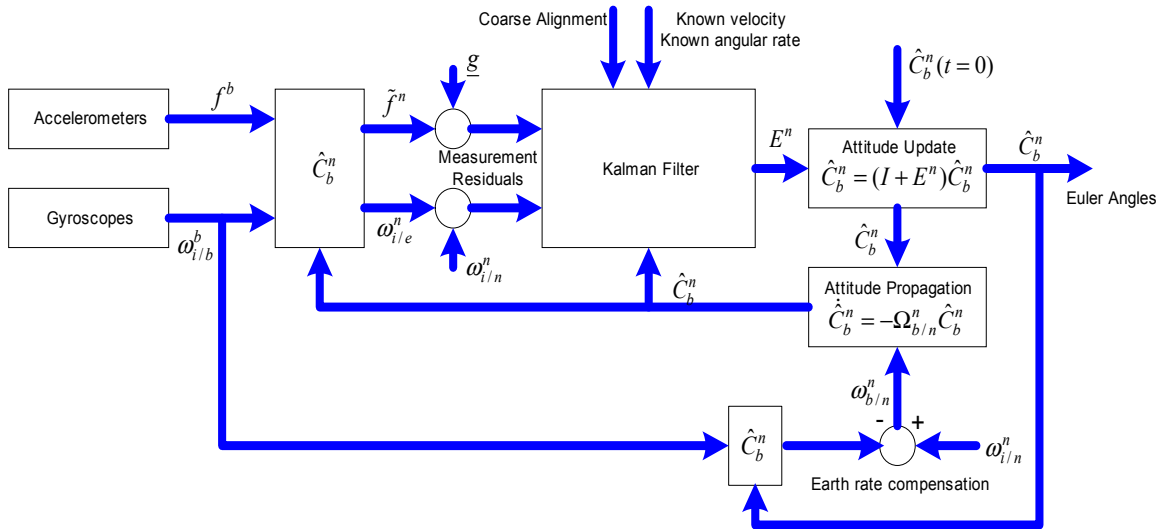


Figure 2. Initial Alignment Block Diagram

3. FREQUENCY ANALYSIS OF DMARS-I-N

The initial alignment test was done using Inertial Science’s DMARS-I-N. In order to determine the autocorrelation time constant of DMARS-I-N, the frequency domain transformation was done. First we designed the low-pass filter to eliminate the high frequency noise. The Chebyshev 6 pole type II low-pass filter was used.

$$|H(f)| = \frac{1}{\sqrt{1 + \epsilon^2 C_n^2(f/f_b)}} \quad (11)$$

The selecting of the cut-off frequency is a design parameter. By selecting the proper cut-off frequency, the high frequency noise and bias noise are divided because the bias noise is basically low frequency noise. Figure 3 shows the gyro X-axis output in the frequency domain and time domain. We know that after passing through the low-pass filter, the high frequency noise was eliminated. Figure 4 shows the autocorrelation functions of gyroscope Y-axis. Above figure is the autocorrelation function of low-pass IMU output, and below figure is the autocorrelation function of raw IMU output. If we assume that the high frequency white noise was eliminated, we can assume that the low-pass autocorrelation function represents the autocorrelation function of the bias noise. The accelerometer autocorrelation function is calculated by the same process. The autocorrelation time constants are calculated using following equation.

$$R_x(\tau) = \sigma^2 e^{-\beta|\tau|} \quad (12)$$

The autocorrelation time constants of DMARS-I-N were determined as follow,

$$\begin{aligned} \tau_a &= 300 \text{ seconds} \\ \tau_g &= 750 \text{ seconds} \end{aligned}$$

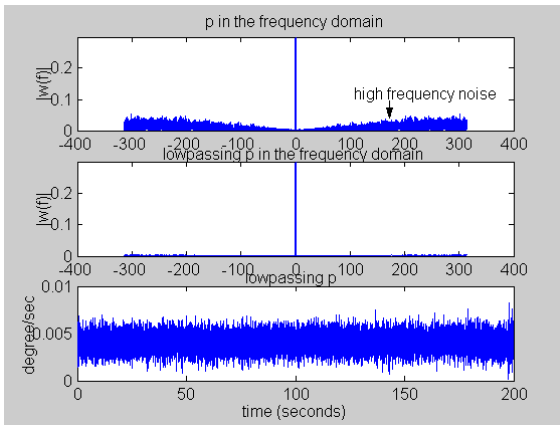


Figure 3. Low pass gyro X-axis output

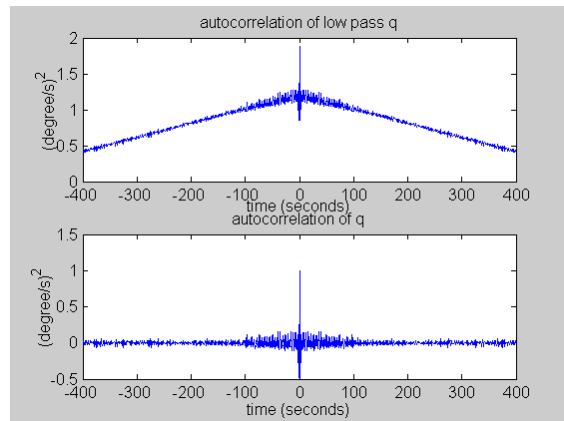


Figure 4. The autocorrelation functions of Gyro Y-axis

4. ADDITIVE BIAS ESTIMATION METHOD

In practice, the real IMU has the constant bias and turn-on bias components. In general, there are number of methods to compensate for the turn-on bias. The first method is to use the Kalman filter in order to estimate turn-on bias [16]. But as stated in Section 1, it is impossible to estimate the turn-on bias in the low cost IMU. Second method is to calibrate the bias in the laboratory [9]. When the IMU axis coincides with the local NED frame, by several rotations, we can calculate the bias magnitude. But this method is limited to the laboratory when we can set the real north direction and real horizon plate. Third method is called the transfer alignment. This method uses the outer reference heading angle [17]. The fourth method is the field calibration [5]. This method uses the least square method to figure out the bias component in accelerometer and gyroscopes by using the known latitude and earth rotation rate in NED frame. During the initial alignment process, the turn-on biases of gyroscope X-axis and Y-axis are main consideration. So, without the constraints that relate gyroscope X-axis with Y-axis, it is hard to estimate the bias components of X-axis and Y-axis in the field calibration method.

In this paper, we suggest a simpler method. We assume that the IMU lies on the horizontal plane. If we ignore the small tilt angles, the gyroscope Z-axis output (\tilde{w}_z^b) is equal to the earth rotation rate corresponding to the downward rotation rate at that latitude as follows.

$$\tilde{w}_z^b = -w_{ie} \sin \lambda + B_z + R_z \quad (13)$$

where B_z is the bias on the gyro Z-axis, and R_z is the random walk noise on the gyro Z-axis. If we use the relatively short period high-pass (approximately 2~3 minutes) IMU data after turn-on, we can ignore the random walk noise component. So the turn-on bias of Z-axis is approximated as follow,

$$B_z = \tilde{w}_z^b + w_{ie} \sin \lambda \quad (14)$$

It is not easy to estimate X-axis and Y-axis bias components in the stationary state. But when the gyroscope rotates, we can estimate by simple method given as follows. Measured earth rotation rate in IMU body axis before the rotation is given as

$$\tilde{w}_{x1} = w_{ie} \cos \lambda \cos(\varphi) + B_x + R_{x1} \quad \text{and} \quad \tilde{w}_{y1} = w_{ie} \cos \lambda \cos(\varphi + 90^\circ) + B_y + R_{y1} \quad (15)$$

Measured earth rotation rate in IMU body axis after the rotation is given as

$$\tilde{w}_{x2} = w_{ie} \cos \lambda \cos(\varphi + \alpha) + B_x + R_{x2} \quad (16)$$

$$\tilde{w}_{y2} = w_{ie} \cos \lambda \cos(\varphi + 90^\circ + \alpha) + B_y + R_{y2} \quad (17)$$

By Eqs. (15-17), below relations are derived.

$$\cos(\varphi + \alpha) - \cos \varphi = \frac{\tilde{w}_{x2} - \tilde{w}_{x1}}{w_{ie} \cos \lambda} \quad \text{and} \quad -\sin(\varphi + \alpha) + \sin \varphi = \frac{\tilde{w}_{y2} - \tilde{w}_{y1}}{w_{ie} \cos \lambda} \quad (18)$$

Eq. (18) can be rewritten as follow,

$$-2 \cdot \sin\left(\varphi + \frac{\alpha}{2}\right) \sin \frac{\alpha}{2} = \frac{\tilde{w}_{x2} - \tilde{w}_{x1}}{w_{ie} \cos \lambda} \quad \text{and} \quad -2 \cdot \cos\left(\varphi + \frac{\alpha}{2}\right) \sin \frac{\alpha}{2} = \frac{\tilde{w}_{y2} - \tilde{w}_{y1}}{w_{ie} \cos \lambda} \quad (19)$$

Let $\frac{\tilde{w}_{x2} - \tilde{w}_{x1}}{w_{ie} \cos \lambda} = a$, and $\frac{\tilde{w}_{y2} - \tilde{w}_{y1}}{w_{ie} \cos \lambda} = b$. By dividing two equations in Eq. (19), the following relation between the rotation

angle and initial azimuth angle is derived.

$$\varphi + \frac{\alpha}{2} = \tan^{-1}\left(\frac{a}{b}\right) \quad (20)$$

Let $\tan^{-1}\left(\frac{a}{b}\right) = c$. If Eq. (20) is substituted into Eq. (16), the initial azimuth angle is derived,

$$\varphi = c - \sin^{-1}\left[\frac{a}{-\sin c}\right] \quad (21)$$

By substituting this initial azimuth angle into Eq. (15), X-axis bias and Y-axis bias are estimated. But because we ignored the random walk noise, the following three conditions have to be satisfied.

- 1) The rotation angle, A , calculated by Eqs. (16) and (20) should be equivalent to the rotation angle, B , which is calculated by the attitude navigation equation using the IMU output data during the rotation period.
- 2) The initial azimuth angle, C , calculated by substituting Eq. (20) into Eq. (16) should be equivalent to the initial azimuth angle, D , calculated by Eqs. (20) and (17).
- 3) The gyro Z-axis outputs after the rotation is equal to Z-axis outputs before the rotation.

But in actual application, above three conditions are difficult to satisfy. So we used the IMU data when the following conditions were satisfied after IMU had been rotated more than 90 degrees.

$$\|A - B\| < 5^\circ \quad \text{and} \quad \|C - D\| < 5^\circ \quad (22)$$

5. SIMULATION AND LABORATORY EXPERIMENT

Simulation Test

For the initial alignment verification, first we tested it using simulated IMU model. The constant bias components are assumed to be compensated. The bias in-run stability components are given in the random generation. Random walk noises are made by Gauss-Markov process using the autocorrelation time constant determined in Section 3. The random walk noise standard deviations are determined in the conditions that satisfy the random noises of DMARS-I-N. This random walk noise is driven by the unity white noise as shown in Section 2. It is important to consider the random measurement white noise. In order to consider the white noises, when the gyroscope senses the earth rotation rate given as $w_{ie} \cos \lambda \cos \varphi$, the measured gyroscope output is given as $w_{ie} \cos \lambda \cos \varphi \pm w_{ie} \cos \lambda \cos \varphi \cdot u(t)$, where $u(t)$ is unity Gaussian white noise. Initial 7 degree azimuth error and 0.5 degree tilt error are assumed.

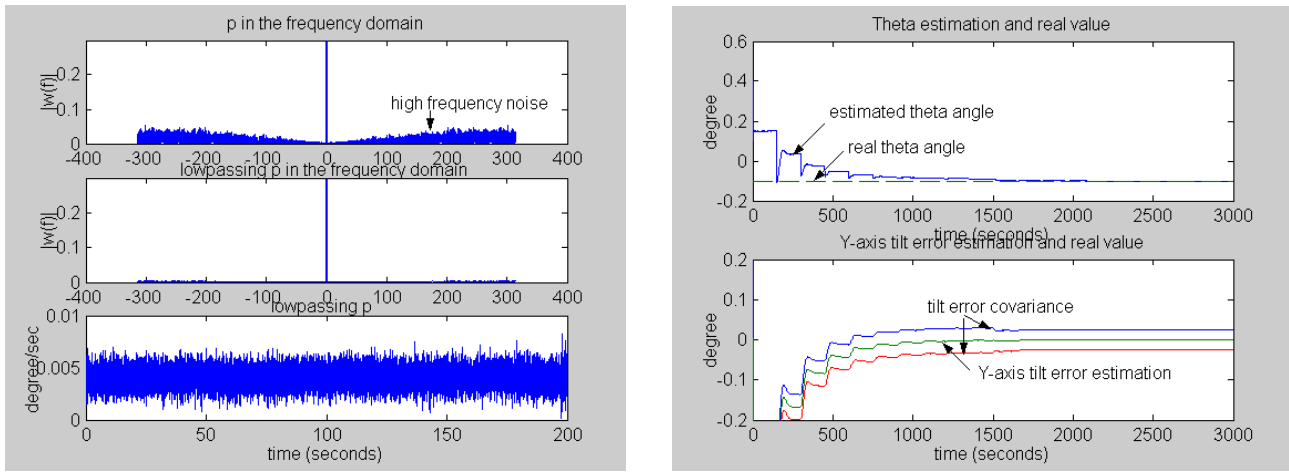


Figure 5.1 X-axis tilt error estimation and Euler Phi angle Figure 5.2 Y-axis tilt error estimation and Euler Theta angle

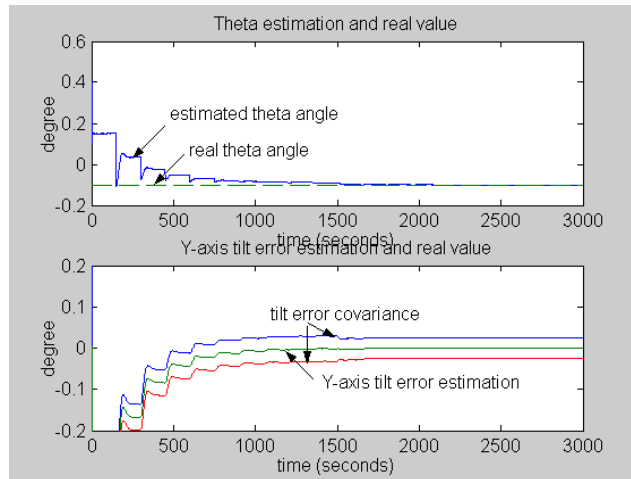


Figure 5.3 Z-axis azimuth error estimation and Euler Psi angle

The process is divided into two different steps. In the first step, the tilt error is estimated. This process is called the 'Leveling' process. As the second step, after 'Leveling' process is complete, the azimuth error is estimated. This process is called, 'Gyro-compassing'. After these two steps are finished, the Euler angle is estimated. Note that, because the azimuth error does not converge well, we used the smoothing method. Figure 5.1 shows the results for the estimation of initial X-axis Euler angle, and Figure 5.2 shows the results for the Y-axis. Figure 5.3 shows the results of Z-axis azimuth angle estimation. From the covariance of Figure 5.1 and 5.2, we know that tilt angles were estimated within 0.02 degree. From the covariance of Figure 5.3, the azimuth angle was estimated within 0.4 degree. But when the estimated Euler angles are compared with the known Euler angles, we knew that the initial attitude angle was estimated within 0.005 degree. Note that (1) when measurement noise covariance was tuned manually, the convergence duration of tilt angle was similar but the azimuth convergence duration took longer than the adaptive method. (2) By manual tuning method, it was very difficult to find the optimal measurement noise covariance matrix. (3) The 200 seconds simulation data were used in smoothing process. So when the IMU data are used again by smoothing method, the innovation matrix of adaptive filter [4] has to be counted again.

DMARS-I-N Laboratory Test

DMARS-I-N was tested by two different experiments. First, a leveling test was done to determine whether IMU senses the true horizon or not. In order to set the true horizon, Ideal Aeromith's rate table and digital level, WYLER MINILEVEL NT, were used. Figure 6 shows the IMU test on the rate table set to true horizon. In order to determine whether DAMAR-I-N finds the true horizon or not, rate table was rotated repeatedly after turn-off and turn-on. Figure 7 shows the test results of the gyro Y-axis. About -0.011 degree (in Figure 7, estimated angle is between -0.006 degree and -0.016 degree) was estimated as an average value of the Y-axis tilt angle. Because IMU was tested after turn-on repeatedly, it is analyzed that -0.011 degree came from the error sources such as the misalignment of IMU platform frame from the body frame, rate table errors, and MINILEVEL bias. So if we compensate -0.011 degree in Y-axis, we can say that IMU Y-axis tilt angle was determined within 0.01 degree ($-0.006 + 0.016 = 0.01$) accuracy. By the same process, the X-axis tilt angle was determined within 0.01 degrees. But the covariance results in Figures 7 shows that tilt error was estimated within 0.03 degree.

Second, the gyro-compassing test was done on the laboratory floor to determine whether the alignment algorithm calculates the initial azimuth angle or not. Because the true north direction was not known, we performed the test repeatedly to verify the precision of the algorithm. Because IMU was tested repeatedly after turn-off and turn-on, if the

bias components were compensated, the alignment results should be the same. Bias components were compensated by the method in Section 4. In order to reduce the random walk noise components, about 3 minutes of high-pass data were used. Before IMU data were used in the Kalman filter, the IMU white noises had to pass the low-pass filter and random infinity impulse noises had to be eliminated by manual method. Figure 8.1 shows the azimuth angle estimations. As shown in figure, alignment algorithm estimates the azimuth angle differently.

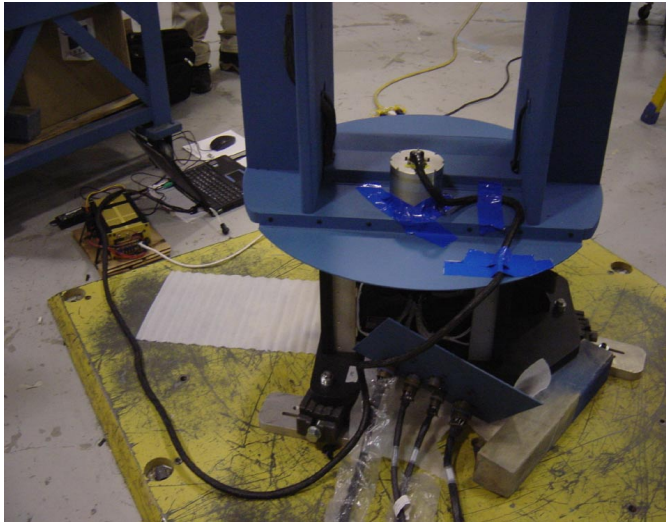


Figure 6. Leveling test using rate table

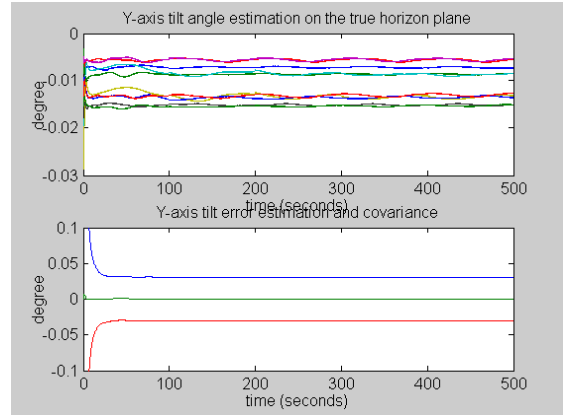


Figure 7. Y-axis tilt angle estimation on the true horizon

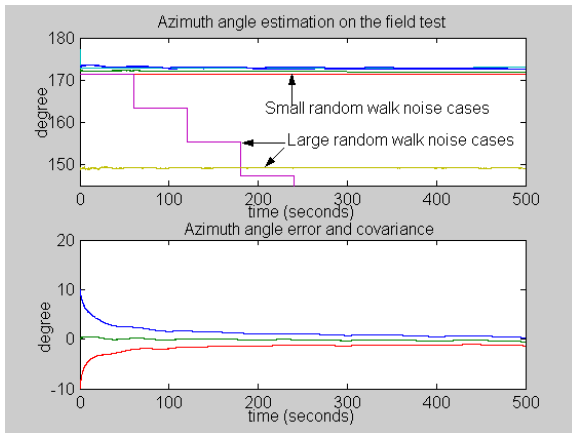


Figure 8.1 Azimuth angle estimation on the floor

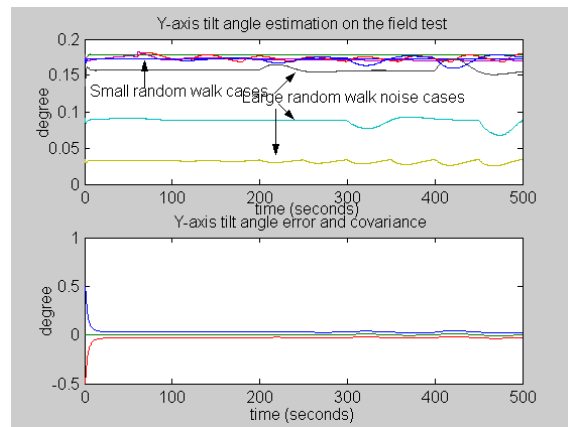


Figure 8.2 Y-axis tile angle estimation on the floor

Because we cannot measure the random walk noise, when Eq. (22) is satisfied, we assume that random walk noise is small. When random walk noise is small, the alignment algorithm estimates the azimuth angles with about 2 degrees angle difference. But when random walk noise is large (i.e., when Eq. (22) is not satisfied), the estimated azimuth angle diverges or the coarsely aligned azimuth angle is estimated with large errors. This also happens during the tilt angle estimation.

The covariance results in Figures (8.1-8.2) show that azimuth angle was estimated within 1 degree error, and tilt angle was estimated within 0.03 degrees. Note that, in Eq. (22), the limiting value of 5 degrees can be changed according to the required design accuracy and IMU performance. Experimental test of DMARS-I-N shows that, when the calculated angle difference in Eq. (22) is less than 5 degrees, azimuth angle is estimated within 2 degrees difference. This 2 degree error of azimuth angle satisfies the required design accuracy as an initial coarse azimuth angle of AEROCam [20].

6. CONCLUSIONS

Experimental results show that for DMARS-I-N, when the bias components are compensated, a gyro-compassing process finds azimuth angle within 2 degrees, and leveling process finds tilt angle within 0.03 degree. When the simulated IMU data are used, an alignment algorithm finds the initial attitude angle more stably (within 0.4 and 0.02 degree). When the actual IMU data are used, because the bias components have to be compensated, initial angles are found under special conditions. Thus we conclude that the calibration accuracy of the additive bias components dominates the initial alignment. From the simulation and the DMARS-I-N test, the adaptive filtering was proved to be effective in calculating the measurement error covariance without tuning the noises. By using a low-pass filter, the autocorrelation time constant of bias noise was calculated. This autocorrelation time constants have been used in Gauss-Markov process. Even though three critical conditions are required, the suggested bias calibration method is simple, and it can be used as a secondary calibration method in AREOCam system.

7. ACKNOWLEDGEMENTS

The authors wish to acknowledge the support of Ideal Aerosmith engineers, Gary Kleven, Lyle Heinsen, Jim Richtsmeier, and Brian Stonecipher. This project was supported through NASA Grant NAG13-01006, "Northern Great Plains Center for People and the Environment," Dr. George A. Seielstad, Principal Investigator, Dr. Leigh Welling, Co-Principal Investigator.

REFERENCES

- [1] Robert M. Rogers, *Applied Mathematics in Integrated Navigation Systems*, AIAA, 2000.
- [2] Robert M. Rogers, 'IMU In-Motion Alignment without Benefit of Attitude Initialization', *ION 1997 National Technical Meeting*—"Navigation and Positioning in the Information Age", January 14-16, 1997.
- [3] Robert M. Rogers, "Low Dynamic IMU Alignment", *IEEE Position Location and Navigation Symposium*, 1998.

- [4] Oleg Salychev, *Inertial Systems in Navigation and Geophysics*, Bauman MSTU Press, MOSCOW, 1998.
- [5] Eun-Hwan Shin, "Accuracy Improvement of Low Cost INS/GPS for Land Applications", Master Thesis, Department of Geomatics Engineering, University of Calgary, 2001.
- [6] Jay A. Farrell, Matthew Barth, *The Global Positioning System & Inertial Navigation*, McGraw-Hill, 1998.
- [7] Eduardo Nebot, Hugh Durrant-Whyte, "Initial calibration and alignment of Low cost Inertial Navigation Units for land vehicle applications", *Journal of Robotics System*, Vol. 16, No. 2, 1999, pp. 81-92.
- [8] J. Aranda, J. M. De La Cruz, S. Dormido, P. Ruiperez, R. Hernandez, "Reduced-order Kalman Filter for Alignment", *Cybernetics and Systems: An International Journal*, Vol. 25, 1994. pp. 1-16.
- [9] Anthony Lawrence, *Modern Inertial Technology*, Springer, 1998.
- [10] Kenneth R. Britting, *Inertial Navigation System Analysis*, Wiley Interscience, 1971.
- [11] Mohinder S. Grewal, Lawrence R. Weill, Angus P. Andrews, *Global Positioning systems, Inertial Navigation and Integration*, Wiley Interscience, 2001.
- [12] Robert Grover Brown, Patrick Y.C. Hwang, *Introduction to Random Signals and applied Kalman Filter*, John Wiley & Sons, 1997.
- [13] Jiang Cheng Fang, De Jun Wan, "A Fast Initial Alignment Method for Strapdown Inertial Navigation System on Stationary Base", *IEEE Transactions on Aerospace and Electronic Systems*, Vol. 32, No. 4, 1996.
- [14] John Baziw, Cornelius T. Leondes, "In-Flight Alignment and Calibration of Inertial Measurement Units-Part I: General Formulation", *IEEE Transactions on Aerospace and Electronic Systems*, Vol. AES-8, No. 4, 1972.
- [15] John Baziw, Cornelius T. Leondes, "In-Flight Alignment and Calibration of Inertial Measurement Units-Part II: Experimental Results", *IEEE Transactions on Aerospace and Electronic Systems*, Vol. AES-8, No. 4, 1972.
- [16] Mohinder S. Grewal, Vinson D. Henderson, Randy S. Miyasako, "Application of Kalman Filtering to the Calibration and Alignment of Inertial Navigation System", *IEEE Transaction on Automatic Control*, Vol. 34, No. 1, 1991.
- [17] Sherryl H. Stovall, "Transfer Alignment", Naval Air Warfare Center Weapons Division, China Lake, CA, 1996.
- [18] Arthur Gelb, *Applied Optimal Estimation*, The MIT Press, 1984.
- [19] Jan Skaloud, 'Optimizing Georeferencing of Airborne Survey Systems by INS/DGPS', The University of Galgary, 1999.
- [20] Peter Osburnsen, 'Design of A GPS/INS Subsystem with KALMAN Estimation for AEROCAM-The Airborne Environmental Research Observational Camera', University of North Dakota, 2002.
- [21] Brian L. Stevens, Frank L. Lewis, *Aircraft Control and Simulation*, Wiley-International, 1992.
- [22] Bong Wie, *Space Vehicle Dynamics and Control*, AIAA Education Series, 1998.
- [23] Leon W. Couch, *Digital and Analog Communication System*, Prentice Hall, 2001.
- [24] E. Bryson, Jr, Yu-Chi Ho, *Applied Optimal Control*, Hemisphere Publishing Corporation, 1975.